

# Observation and Control of Interfacial Defects in ZnO/ZnSe Coaxial Nanowires

W.A. BHUTTO, Z.M. WU\*, Y.Y. CAO, W.P. WANG AND J.Y. KANG\*

Fujian Key Laboratory of Semiconductor Materials and Applications, Department of Physics, Xiamen University  
Xiamen 361005, P.R. China

ZnO/ZnSe coaxial nanowires with different ZnO core diameters were synthesized by using a two-step chemical vapor deposition. The scanning electron microscopy images demonstrated that the coaxial nanowires with small ZnO core diameter had the smoother surface than that with large ZnO core diameter. A coherent ZnSe layer with wurtzite structure was observed in the nanowire interface between the ZnO core and the ZnSe shell by high resolution transmission electron microscopy. This coherent layer is beneficial to reduce the defect density and improve the crystal quality by suppressing the phase transition. It was found that the coherent thickness was significantly related to the ZnO core diameter. For the nanowire with large ZnO core, a thin critical thickness of 2–3 nm was obtained. As a result, a layer of zinc blende ZnSe appeared outside the nanowire, and a lot of defects existed in the interface between the ZnSe layers with different phase structures. For the nanowire with small ZnO core, however, the critical thickness increased and a coherent coaxial structure was observed with the same lattice spacing in the ZnO core and the ZnSe shell. To obtain defect-free coaxial nanowire, an optimal structure was also proposed by theoretical calculation.

DOI: [10.12693/APhysPolA.125.994](https://doi.org/10.12693/APhysPolA.125.994)

PACS: 62.23.Hj, 61.46.Km, 64.70.Nd, 68.35.Ct

## 1. Introduction

Nowadays, one-dimensional semiconductor nanomaterials have attracted much attention due to their potential applications in nanoelectronic and nanophotonic devices, such as nanolasers, light emitting diodes, solar cells and so on [1–6]. Among the semiconductor materials, zinc oxide (ZnO) obtains considerable research interests due to its mature one-dimensional growth technology and wide bandgap (3.37 eV) as well as large exciton binding energy (60 meV) [7, 8]. Recently, varieties of ZnO-based coaxial nanowires (NWs), such as ZnO/ZnSe, ZnO/ZnS, ZnO/ZnTe, have been synthesized to control and enhance their functions [9–13]. As we know, interfacial structure and quality play important role in structural material performances. It is expected to grow coherently coaxial nanowire without interfacial defects. Different methods have been attempted to make high quality heterostructures [14–17], but it is still a challenge because of the lattice mismatch between the core and the shell, especially for ZnO/ZnSe with larger mismatch [18].

In this work, we aim to grow ZnO/ZnSe core/shell nanowires with high quality interface by using a two-step chemical vapor deposition (CVD). Different diameters of ZnO cores were synthesized to investigate the relation between the defects and the lattice misfit strain. The morphologies were characterized by scanning electron microscopy (SEM). The interface structures and critical thickness were examined by high-resolution transmission electron microscopy (HRTEM). Finally, an optimized coaxial structure was suggested based on the theoretical analysis.

## 2. Experimentals

The growth of vertically well-aligned ZnO NWs on aluminum zinc oxide (AZO) substrate was carried out in a horizontal quartz tube furnace with three heating zones. Zinc powder (4N, 1 g) was used as the source material and placed at the central heating zone of quartz tube. The substrate with the dimensions of 1 cm × 1 cm was placed at a distance of 8 cm downstream of the Zn powder. Before heating, the system was evacuated to  $1.0 \times 10^{-2}$  Pa, and a mixed gas consisting of 100 sccm N<sub>2</sub> flow and 8 sccm O<sub>2</sub> flow was introduced into the tube. Then, the tube was heated to 580 °C at a rate of 20 °C/min and kept at this temperature for 30 min.

The diameter and density of nanowires were controlled by the distance between substrate and source. After the growth, the tube furnace was cooled down to room temperature and then high purity Se powder (5N, 0.2 g) was placed at the first zone, upstream of the Zn powder, to grow the ZnSe shell. Subsequently, the system was evacuated again and then only 200 sccm N<sub>2</sub>, as a carrier gas, was flowed through the tube. The heating zones were heated at a rate of 20 °C/min. During the ZnSe shell growth, the temperature of the first zone was kept at 420 °C while the central zone at 620 °C. After 120 min growth, the system was naturally cooled down to room temperature. Morphologies of the as-grown ZnO and ZnO/ZnSe NWs were characterized by a field emission SEM (LEO 1530). The structures and compositions were analyzed by a field emission TEM (Tecnai F30) and energy-dispersive X-ray spectroscopy (EDS), respectively.

## 3. Results and discussion

The morphologies of ZnO/ZnSe nanowires with different ZnO diameters were observed by SEM. Figure 1 shows that NWs are uniform and vertical to AZO sub-

\*corresponding author; e-mail:

[zmwu@xmu.edu.cn](mailto:zmwu@xmu.edu.cn), [jkang@xmu.edu.cn](mailto:jkang@xmu.edu.cn)

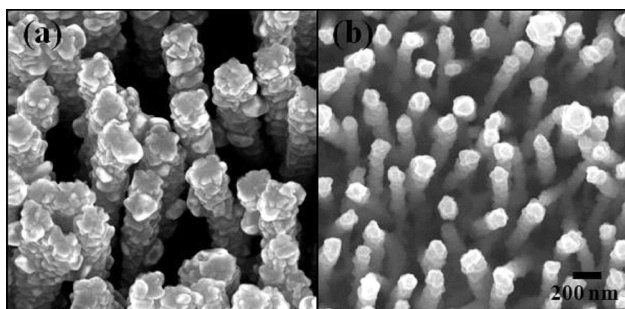


Fig. 1. SEM images of ZnO/ZnSe NWs with large (a) and small (b) diameters.

strate. The NWs with large diameters have rough surface as shown in Fig. 1a, while that with small diameters have relatively smooth surface as observed in Fig. 1b. The different roughness may be due to their different internal structures.

To further analysis of their structures, the coaxial NWs with different diameters were characterized by TEM, as shown in Fig. 2a and b. An obvious contrast difference appears between the core and the shell in Fig. 2a, confirming the formation of the core/shell structure. Figure 2c shows the EDS line-scan profile across the nanowire in Fig. 2a. Only three characteristic peaks of Zn, O, and Se elements are observed. The Zn element appears in both the core and shell region, and the O element only appears in the core region, demonstrating the ZnO core. In addition, there are two Se peaks displaying in the shell regions, confirming the formation of ZnSe compounds in the shell layer. Compared with the coaxial NW in Fig. 2a, the thinner NW in Fig. 2b has the relatively uniform contrast, revealing the different internal structure. To understand the structural difference, HRTEM was conducted to image the cross-sections, particularly at interface. Figure 2d,e illustrates the images of the interfaces between ZnO core and ZnSe shell for the nanowires in Fig. 2a and b, respectively. For the ZnO/ZnSe NWs with large ZnO core diameter, three distinct regions can be recognized, as demonstrated in Fig. 2d. ZnO core region exhibits structural features of wurtzite (WZ) phase structure in  $\langle 0001 \rangle$  directions. Detailed examination shows that the lattice spacing of 0.260 nm is slightly larger than that of bulk WZ ZnO, which is attributed to the lattice deformation caused by misfit strain between ZnO core and ZnSe shell. On the outer side of ZnO core, two regions with different lattice features are distinguished, which correspond to ZnSe shell due to their similar contrast differing from that of ZnO core.

By comparing the lattice spacing, the region close to the core has a lattice spacing of 0.260 nm, the same as that of ZnO, indicating that the WZ ZnSe shell has been coherently grown on ZnO lateral surface. Additionally, another ZnSe region far from ZnO core has a lattice spacing of 0.327 nm, corresponding to zinc blende (ZB) structure of ZnSe along the  $\langle 111 \rangle$  directions. However, only

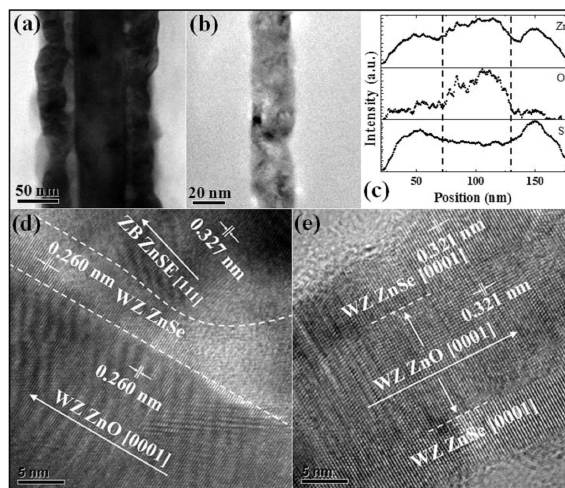


Fig. 2. Low-magnification TEM images of ZnO/ZnSe NWs with large (a) and small (b) core diameters. (c) EDS line-scan profiles of the elements Zn, O, and Se across the nanowire in (a). (d) and (e) High-resolution TEM images of the interface between the ZnO core and the ZnSe shell for the nanowires in (a) and (b).

former two regions appear in the ZnO/ZnSe NWs with small core diameter and have the same lattice spacing of 0.321 nm and structural features, as shown in Fig. 2e. This spacing value is much larger than that of bulk ZnO but smaller than that of bulk ZnSe in  $\langle 0001 \rangle$  directions because the misfit stress between ZnO core and ZnSe shell has been accommodated by the elastic strain. It is interested to note that the nanowire with large ZnO core, as shown in Fig. 2d, has many defects in the interface between the ZnSe layers with different phase structures due to the large lattice mismatch. To relieve the misfit stress, many crystal grains are formed in the outside layer of ZB ZnSe and an obvious rotation of ZB ZnSe crystal direction  $\langle 111 \rangle$  against WZ ZnSe  $\langle 0001 \rangle$  occurs. As a result, the surface of coaxial nanowire becomes rough, as illustrated in Fig. 1a. However, for the nanowire with small ZnO core, the interface between the core and the shell is almost defect-free due to the coherent structure. Meanwhile, the surface of coaxial nanowire is relatively smooth compared to large ZnO core. This is because most of the misfit stress is accommodated in the ZnO core, instead of the ZnSe shell.

It has been known that there is a large mismatch between ZnO core and ZnSe shell, and phase transition occurs when the shell thickness is beyond a critical value. The detailed HRTEM analysis indicates that misfit defect density increases with the increase of layer thickness. To reduce defect density by suppressing the phase transition, ZnSe shell should be grown within the critical thickness to accommodate the large misfit strain by elastic deformation. According to the TEM investigation, the critical thickness of the ZnSe is also related to the diameter of ZnO core.

In the light of this investigation, we constructed a cylindrical ZnO/ZnSe core/shell nanowire model, as

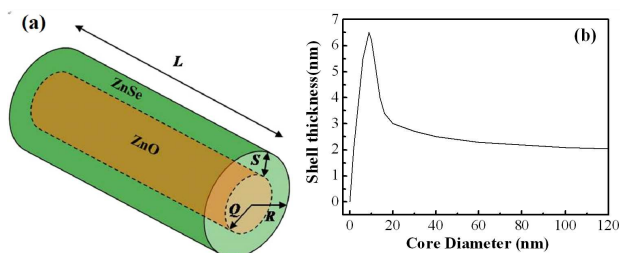


Fig. 3. (a) Schematic of a ZnO/ZnSe core/shell NWs, (b) critical thickness of coherent ZnSe layer for different ZnO core diameter.

shown in Fig. 3a, to examine the dependence of critical thickness on the ZnO core diameter. The axis of the wire is assumed to be along the  $\langle 0001 \rangle$  directions of WZ structure. The strained structures of ZnO/ZnSe core/shell nanowires were investigated by mechanic equilibrium method, and the coherent critical thickness of ZnSe was determined by the formation of misfit dislocations and crystalline phase transition [19].

As it can be seen in Fig. 3b, when ZnO diameter is larger than 20 nm, the critical thickness is very thin, about 2–3 nm, which agrees well with the observation in Fig. 2a. Let us note that it dramatically increases with the decrease of core diameter. Generally, an unlimited critical thickness is expected for the core/shell nanowire, such as Si/Ge [20], when the core diameter tends to be zero. However, an optimal critical value of 6.5 nm is obtained at ZnO core diameter of 9 nm in ZnO/ZnSe core/shell nanowire. This anomalous phenomenon is because of the large lattice mismatch (up to 27%) that results in the occurrence of phase transition or defect appearance in ZnO core when the thickness of ZnSe shell is beyond the optimal value [21]. Hence, to obtain a defect-free ZnO/ZnSe core/shell nanowire, not only the thickness of ZnSe shell but also the diameter of ZnO core should be well controlled.

#### 4. Conclusion

In summary, we performed a two-step CVD method to grow ZnO/ZnSe coaxial nanowires with different ZnO core diameters. Morphological studies by SEM demonstrated that the coaxial NWs with small ZnO core diameter had relatively smooth surface. TEM results revealed that a coherent ZnSe layer with wurtzite structure was preferential to grow outside the ZnO core. This coherent layer is beneficial to reduce the defect density and improve the crystal quality by suppressing the phase transition. Meanwhile, this coherent thickness significantly depends on the ZnO core diameter. For the nanowire with large ZnO core diameter, the critical thickness is thin, and a layer of zinc blende ZnSe appears outside the nanowire, resulting in an increase of defects in the interface between the ZnSe layers with different phase structures. While for the nanowire with the small ZnO core, a coherent coaxial structure was observed with the same lattice spacing in the ZnO core and the ZnSe shell. Finally, to obtain defect-free coaxial nanowire, an optimal structure with ZnO core of about 9 nm in diameter

and ZnSe shell of 6.5 nm in thickness was proposed by theoretical calculation.

#### Acknowledgments

The work was supported by “973” Program (No. 2012CB619301 and 2011CB925600), the National Natural Science Foundations of China (No. 61106008 and 61227009), the Natural Science Foundations of Fujian Province, and the fundamental research funds for the central universities (No. 2011121042).

#### References

- [1] K. Suenaga, C. Colliex, N. Demoncy, A. Loiseau, H. Pascard, F. Willaime, *Science* **653**, 278 (1997).
- [2] Y. Zhang, K. Suenaga, C. Colliex, S. Iijima, *Science* **281**, 973 (1998).
- [3] Z.M. Wu, Y. Zhang, J.J. Zheng, X.G. Lin, X.H. Chen, B. Huang, H.Q. Wang, K. Huang, S.P. Li, J.Y. Kang, *J. Mater. Chem.* **21**, 6020 (2011).
- [4] A.I. Hochbaum, P.D. Yang, *Chem. Rev.* **110**, 527 (2010).
- [5] B. Hua, J. Motohisa, Y. Kobayashi, S. Hara, T. Fukui, *Nano Lett.* **9**, 112 (2009).
- [6] O. Hayden, A.B. Greytak, D.C. Bell, *Adv. Mater.* **17**, 701 (2005).
- [7] W.J.E. Beek, M.M. Wienk, R.A.J. Janssen, *Adv. Mater.* **16**, 1009 (2004).
- [8] J.J. Zheng, Z.M. Wu, W.H. Yang, S.P. Li, J.Y. Kang, *J. Mater. Res.* **25**, 1272 (2010).
- [9] Y. Zhang, J. Pern, A. Mascarenhas, W.L. Zhou, *SPIE Newsroom* **11**, 1388 (2008).
- [10] K. Wang, J.J. Chen, W.L. Zhou, Y. Zhang, Y.F. Yan, J. Pern, A. Mascarenhas, *Adv. Mater.* **20**, 3248 (2008).
- [11] H.Y. Chao, J.H. Cheng, J.Y. Lu, Y.H. Chang, C.L. Cheng, Y.F. Chen, *Superlatt. Microstruct.* **47**, 160 (2010).
- [12] E. Janik, A. Wachnicka, E. Guziewicz, M. Godlewski, S. Kret, W. Zaleszczyk, E. Dynowska, A. Presz, G. Karczewski, T. Wojtowicz, *Nanotechnology* **21**, 015302 (2010).
- [13] K. Wang, J.J. Chen, Z.M. Zeng, J. Tarr, W.L. Zhou, Y. Zhang, Y.F. Yan, C.S. Jiang, J. Pern, A. Mascarenhas, *Appl. Phys. Lett.* **96**, 123105 (2010).
- [14] M.S. Gudiksen, L.J. Lauhon, J. Wang, D.C. Smith, C.M. Lieber, *Nature* **415**, 617 (2002).
- [15] L.J. Lauhon, M.S. Gudiksen, C.M. Lieber, *Math. Phys. Eng. Sci.* **362**, 1247 (2004).
- [16] Y.W. Heo, C. Abernathy, K. Pruessner, W. Sigmund, D.P. Norton, *J. Appl. Phys.* **96**, 3424 (2004).
- [17] L. Pan, K.K. Lew, J.M. Redwing, E.C. Dickey, *Nano Lett.* **5**, 1081 (2005).
- [18] J. Hsueh, *Cryst. Growth* **302**, 258 (2003).
- [19] S. Raychaudhuri, E.T. Yu, *Appl. Phys. Lett.* **99**, 114308 (2006).
- [20] E.T. Trammell, X. Zhang, Y.L. Li, L.Q. Chen, E.C. Dickey, *J. Cryst. Growth* **310**, 3084 (2008).
- [21] Y.P. Wu, X.H. Zhang, F.C. Xu, L.S. Zheng, J.Y. Kang, *Nanotechnology* **20**, 325709 (2009).